Title

Identification and characterization of key kinetic intermediates in amyloid β-protein fibrillogenesis11Edited by F. Cohen

Journal

Journal of Molecular Biology, 312(5)

ISSN

0022-2836

Authors

Kirkitadze, Marina D
Condron, Margaret M
Teplow, David B

Publication Date

2001-10-01

DOI

10.1006/jmbi.2001.4970

Peer reviewed

doi:10.1006/jmbi.2001.4970 available online at http://www.idealibrary.com on IDEAL® J. Mol. Biol. (2001) 312, 1103–1119

JMB

Identification and Characterization of Key Kinetic Intermediates in Amyloid β-protein Fibrillogenesis

Marina D. Kirkitadze, Margaret M. Condron and David B. Teplow*

Center for Neurologic Diseases Brigham and Women's Hospital, and Department of Neurology (Neuroscience) Harvard Medical School Boston, MA 02115, USA

*Corresponding author

Amyloid β-protein (Aβ) assembly into toxic oligomeric and fibrillar structures is a seminal event in Alzheimer's disease, therefore blocking this process could have significant therapeutic benefit. A rigorous mechanistic understanding of Aβ assembly would facilitate the targeting and design of fibrillogenesis inhibitors. Prior studies have shown that Aβ fibrillogenesis involves conformational changes leading to the formation of extended β-sheets and that an α-helix-containing intermediate may be involved. However, the significance of this intermediate has been a matter of debate. We report here that the formation of an oligomeric, α-helix-containing assembly is a key step in Aβ fibrillogenesis. The generality of this phenomenon was supported by conformational studies of 18 different Aβ peptides, including wild-type Aβ(1-40) and Aβ(1-42), biologically relevant truncated and chemically modified Aβ peptides, and Aβ peptides causing familial forms of cerebral amyloid angiopathy. Without exception, fibrillogenesis of these peptides involved an oligomeric α-helix-containing intermediate and the kinetics of formation of the intermediate and of fibrils was temporally correlated. The kinetics varied depending on amino acid sequence and the extent of peptide N- and C-terminal truncation. The pH dependence of helix formation suggested that Asp and His exerted significant control over this process and over fibrillogenesis in general. Consistent with this idea, Aβ peptides containing Asp → Asn or His → Gln substitutions showed altered fibrillogenesis kinetics. These data emphasize the importance of the dynamic interplay between Aβ monomer conformation and oligomerization state in controlling fibrillogenesis kinetics.

Keywords: Alzheimer's disease; fibrillogenesis; amyloid β-protein; protein folding

Introduction

Alzheimer's disease (AD) is the most prevalent age-dependent dementia.[1] AD is characterized pathologically by the accumulation of extracellular amyloid deposits in the cerebral neuropil and vasculature and of intracellular neurofibrillary tangles.[2] Amyloid deposits contain the amyloid β-protein (Aβ), which is a 40-42 residue peptide produced by endoproteolytic cleavage of the amyloid β-protein precursor (AβPP).[3] A compelling body of evidence supports a seminal role for Aβ in AD.[4] In particular, fibrillization of Aβ is associated with a cascade of neuropathogenetic events which produces the cognitive and behavioral decline characteristic of AD.[5] The central role of fibrillar Aβ in AD pathogenesis has stimulated the development of therapeutic approaches designed to prevent fibril formation (for a review, see reference 6) or to dissociate existing fibrils.[7–9] However, recent studies have shown that other types of Aβ assemblies, including small oligomers (ADDLs)[10,11] and fibril intermediates (protofibrils),[12,13] are neurotoxic. Agents which dissociate fibrils to produce these smaller, yet toxic, species may thus not be of value. In order to rationally develop efficacious therapeutic agents, a rigorous understanding of Aβ assembly is required. Knowledge of early conformational and associative events would allow the targeting of critical steps in the fibrillogenesis pro-

Abbreviations used: Aβ, amyloid β-protein; AD, Alzheimer's disease; CAA, cerebral amyloid angiopathy; TFE, trifluoroethanol; RC, random coil; MWCO, molecular weight cut off; LMW, low molecular weight.

E-mail address of the corresponding author: teplow@cnd.bwh.harvard.edu

0022-2836/01/051103–17 $35.00/0

cess, in particular those leading to the formation of toxic prefibrillar structures.

Amyloid fibrils form by an ordered association of nascent, monomeric Aβ peptides into complex assemblies of polymers. Early studies of amyloid deposits focused on fibril morphology and the primary structure of their Aβ peptide component.[14–16] Tinctorial analysis of the secondary structure of Aβ within these deposits revealed β-sheet structure.[17–19] Fiber X-ray diffraction analyses of *ex vivo* amyloid preparations confirmed and extended these data, revealing a silk-like cross-β pleated-sheet organization of Aβ fibrils.[20] X-ray crystallographic determination of the structure of Aβ within the fibril has not been achieved because of the non-crystalline nature of the assembly. However, *in vitro* solid-state NMR experiments have provided important insight into the organization of β-strands within the fibril.[21] Two areas of recent intense investigation, the conformational transitions associated with the assembly of monomers into fibrils and the identification and characterization of fibril assembly intermediates (for reviews, see references 22-24), have produced important new insights into the fibrillogenesis process. In particular, the identification of neurotoxic, globular Aβ oligomers (ADDLs) and neurotoxic fibril intermediates (protofibrils) has increased the importance of determining the pathway(s) of Aβ folding and assembly.

The conformational states of Aβ at the beginning and end of the fibrillogenesis process are best understood. *In vitro* solution phase NMR studies, done in the absence of organic modifiers such as trifluoroethanol (TFE) or SDS, have shown that monomers of Aβ(10-35)-NH_2, Aβ(1-40), or Aβ(1-42) possess no α-helical or β-sheet structure.[25,26] Aβ(1-40) and Aβ(1-42) exist predominately as random extended chains,[25] whereas the model peptide Aβ(10-35)-NH_2 appears to form an unusual collapsed coil structure composed of loops, strands, and turns.[26] In the presence of TFE or SDS, conditions thought to ''mimic'' the milieu of membrane-associated Aβ, both Aβ(1-40) and Aβ(1-42) are structured, exhibiting predominately α-helical conformations.[27–31] In all cases, following fibril assembly, the Aβ monomer exists in a predominately β-sheet conformation[20,32] within a polymeric peptide assembly. How is this structural transformation accomplished?

AβPP is a type I integral membrane protein whose single transmembrane domain, containing the C-terminal 12-14 residues of Aβ, is postulated to exist in a helical conformation.[33,34] The first 28 residues of Aβ, which compose the C terminus of the AβPP ectodomain, may also be predominately helical. If so, Aβ must undergo an α-helix → β-sheet transition during fibril formation. However, if helix unfolding occurs following Aβ excision, a direct random coil (RC) → β-sheet transition may also occur. Precedents exist in nature for the operation of both pathways. For example, α-synuclein, which in Parkinson's disease forms intraneuronal inclusions termed Lewy bodies,[35] appears to be natively unfolded.[36] Yet, under the appropriate conditions, the protein can assemble into amyloid fibrils[37,38] or fold into a largely helical conformation.[39,40] In contrast, the scrapie prion protein[41,42] and lysozyme[43] have stable native tertiary structures containing a number of α-helices. However, through template-mediated[44] or mutation-induced[43] helix destabilization, both proteins can undergo α-helix → β-strand transitions which lead to amyloid fibril formation.

Conformational studies of Aβ protofibril formation and protofibril maturation into fibrils, done using carefully disaggregated Aβ preparations, have revealed the transitory development of substantial α-helix content.[12] This finding led to the postulation that Aβ fibrillogenesis might involve the formation of a partially helical intermediate which would then undergo further conformational rearrangements to assemble into fibrils.[12] In contrast, earlier work had demonstrated that an Aβ alloform†, [Ala18]Aβ(1-40), with an increased propensity for helix formation, had a decreased ability to form fibrils.[27] This finding led to the conclusion that two stable populations of Aβ monomers existed, a non-helical, β-sheet-containing population ''able'' to fibrillize, and a helix-rich population ''unable'' to do so.[27] If helix formation is indeed ''off-pathway'' for fibrillogenesis, one would seek to facilitate the formation and stabilization of helical regions of the Aβ peptide. However, if the converse were true, this strategy could result in an acceleration of the disease process. Understanding the role of helix formation in Aβ fibrillogenesis is thus important if safe and effective therapeutic approaches are to be developed. We report here results of systematic studies examining the conformational transitions through which Aβ proceeds during fibrillogenesis. These studies demonstrate that helix formation is a key step in Aβ fibril assembly and reveal important mechanistic features of the process. In addition, we discuss the relevance of these findings for understanding the basic principles of amyloid fibril assembly and the etiology of familial forms of amyloidosis.

Results

Structural and kinetic studies of Aβ fibril intermediates

Recently, temporal studies of Aβ conformation during protofibril and fibril assembly have suggested that during the conversion of the unstructured, unassembled Aβ peptide into a β-sheet-rich fibril, a transitory increase in α-helix content occurs.[12] This increase occurs immediately prior to the appearance of the β-sheet structure,

suggesting a precursor-product relationship exists between an α-helix-containing intermediate and a later, β-sheet-rich assembly. We sought to determine whether formation of this intermediate is an obligatory step in Aβ fibrillogenesis, and if so, what factors affect its formation. To do so, circular dichroism spectroscopy (CD) was used to monitor the secondary structure of Aβ during incubation at pH 7.5 and 22 °C. To rule out the possibility that our initial observations resulted from an idiotypic property of Aβ(1-40), 17 additional peptides were studied (Table 1). Each of these peptides was included because of its association with sporadic or familial forms of AD or with cerebral amyloid angiopathy (CAA). These peptides include the majority of the clinically relevant Aβ alloforms thus far described *in vivo*.

To establish a standard for comparison among the 18 peptides, Aβ(1-40) and Aβ(1-42) were studied first. Samples of low molecular weight (LMW) Aβ (monomeric or dimeric)[12] were prepared by the dissolution of lyophilizates in 10 mM glycine buffer (pH 7.5), followed by sonication and filtration (10,000 molecular weight cut off (MWCO)). Immediately after dissolution, Aβ(1-40) was largely unstructured (Figure 1(a)). However, over a period of approximately three weeks, spectra were observed that were consistent first with conformations of mixed α/β character and then with primarily β character. Deconvolution of the

Table 1. Aβ peptides and alloforms

Peptide	Sequence
Aβ(1-42)	DAEFRHDSGYEVHHQKLVFFAEDVGSNKGAIIGLMVGGVVIA
Aβ(1-40)	--
[Gly21]Aβ(1-42) (Flemish)	--------------------G----------------------
[Gly21]Aβ(1-40) (Flemish)	--------------------G-------------------
[Gly22]Aβ(1-42) (Arctic)	----------------------G---------------------
[Gly22]Aβ(1-40) (Arctic)	----------------------G------------------
[Gln22]Aβ(1-42) (Dutch)	----------------------Q---------------------
[Gln22]Aβ(1-40) (Dutch)	----------------------Q------------------
[Lys22]Aβ(1-42) (Italian)	----------------------K---------------------
[Lys22]Aβ(1-40) (Italian)	----------------------K------------------
Aβ(3-42)	---------------------------------------
Aβ(3-40)	---------------------------------------
[<E3]Aβ(3-42)	<E-------------------------------------
[<E3]Aβ(3-40)	<E----------------------------------
Aβ(11-42)	----------------------------------
Aβ(11-40)	------------------------------
[<E11]Aβ(11-42)	<E----------------------------------
[<E11]Aβ(11-40)	<E------------------------------
[Asn1]Aβ(1-40)	N--
[Asn7]Aβ(1-40)	------N----------------------------------
[Asn23]Aβ(1-40)	----------------------N------------------
[Gln6]Aβ(1-40)	-----Q----------------------------------
[Gln13]Aβ(1-40)	------------Q----------------------------
[Gln14]Aβ(1-40)	-------------Q---------------------------
[Asn1,7,23]Aβ(1-40)	N-----N---------------N------------------
[Gln6,13,14]Aβ(1-40)	-----Q------QQ---------------------------

The names and sequences (in IUPAC-designated one-letter code) of the peptides used are listed under those of wild-type Aβ(1-42). Dashes indicate identical amino acid residues and blanks indicate missing residues (truncations). Pyroglutamate is signified by <E.

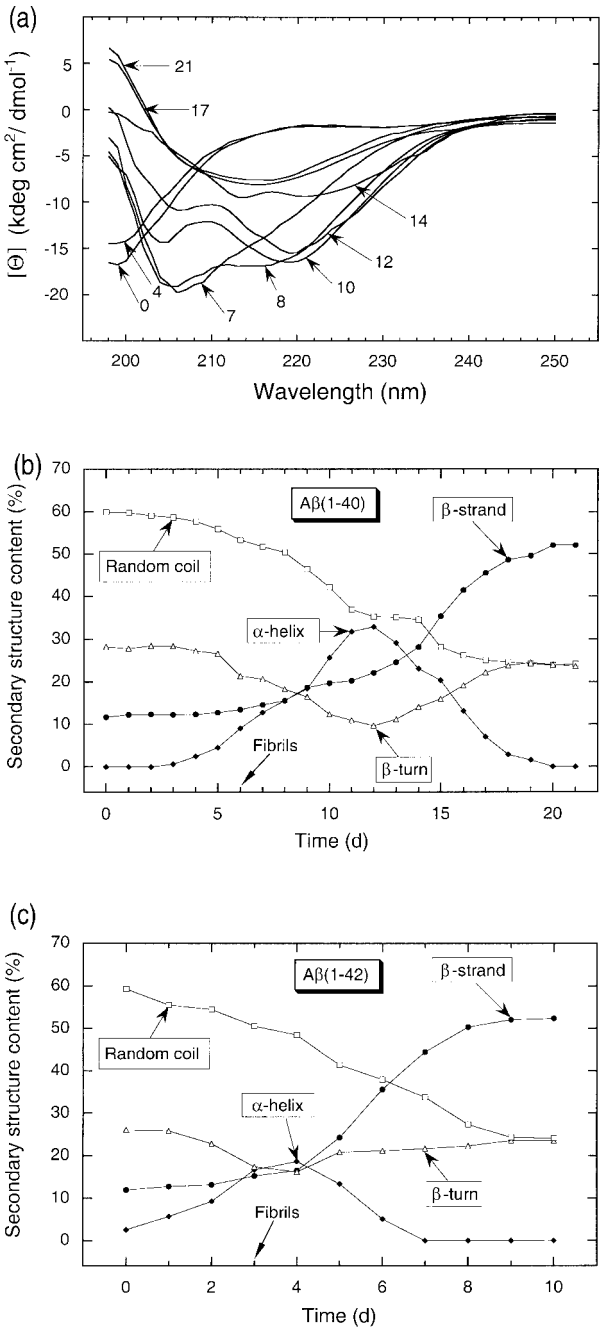

Figure 1. Secondary structure changes of LMW Aβ during fibrillogenesis. (a) LMW Aβ(1-40) was incubated at a concentration of 25-30 μM in 10 mM glycine buffer (pH 7.5) at 22 °C. CD spectra were acquired daily for 21 days (numerals indicate the day of analysis). Results are expressed as molar ellipticity [Θ] (kdeg cm^2 $dmol^{-1}$). The spectra shown are the averages of three scans each with an averaging time of five seconds. These results are representative of those obtained in each of four independent experiments. (b) Each of the daily spectra was deconvoluted, using the program CDANAL[45] and the Brahms and Brahms reference library,[109] to yield the relative amounts of random coil, α-helix, β-sheet and β-turn. The percentages of each secondary-structure element were then plotted *versus* time in days (d). The day at which fibril formation was first observed electron microscopically is indicated by the arrow labeled "Fibrils." (c) Aβ(1-42) was prepared and studied as above. These results are representative of those obtained in each of five independent experiments.

initial spectra using the CDANAL algorithm[45] revealed predominately random coil (60 %) and β-turn (28 %) elements, with a small amount of β-sheet (12 %) and negligible α-helix (Figure 1(b)). RC content decreased steadily throughout the incubation period. β-turn content decreased for ~12 days, after which it rose steadily before plateauing at ~23 %. β-strand content remained low for about one week, then rose to >50 % after three weeks. This rise occurred relatively slowly for ~11 days, then a much more rapid increase in β-sheet content was observed. The graphic profile of helix content was Gaussian in shape, exhibiting a maximum of ~32 % at 11-12 days. We refer to the time (day) at which maximal α-helix content is observed as t_{max}, and the percent α-helix at this time as α_{max}. Interestingly, both the nadir of the β-turn curve, and the point at which the most rapid development of β-sheet began, also occurred at 11-12 days. Aβ(1-42) prepared and incubated identically with Aβ(1-40) displayed similar conformational transitions from RC → α-helix → b-sheet (Figure 1(c)) . Relative to Aβ(1-40), the kinetics of Aβ(1-42) fibrillogenesis was significantly accelerated, as maximal helix content was observed at day 4. At this time, the highest level of α-helix was slightly more than half that of Aβ(1-40). To study the morphology of the β-sheet-containing conformers, samples of Aβ(1-40) and Aβ(1-42) were studied by electron microscopy (EM) after 21 days (Figure 2). This analysis revealed helically twisted fibrils of indefinite length and diameters of ~8 nm.

CD analysis generally provides accurate estimations of α-helix content.[46] However, differences in absolute levels of helix can be observed using different deconvolution protocols. In addition, β-turn content can be difficult to assess due to intrinsic variations in turn structure and to the low magnitude of the turn band relative to those from helix and sheets.[47] For these reasons, the spectra from Aβ(1-40) and Aβ(1-42) were also analyzed using the CONTIN/LL deconvolution algorithm.[48] The qualitative and quantitative features of the temporal development and disappearance of α-helix that were revealed were almost identical with those determined using CDANAL (data not shown). For both Aβ(1-40) and Aβ(1-42), the t_{max} values determined by each method for each peptide were identical. The α_{max} values for Aβ(1-40) were also identical (32 %) and the α_{max} values for Aβ(1-42) were similar (19 % (CDANAL) *versus* 24 % (CONTIN/LL)). Also identical was the shape of the function describing the temporal change in β-strand content. In all four cases, i.e. for Aβ(1-40) and Aβ(1-42) deconvoluted with each of the two algorithms, β-strand content rose slowly until the peak of α-helix was observed, after which an exponential increase in strand content was observed. For Aβ(1-40), a difference was observed between the two approaches in the initial level of β-turn found (28 % (CDANAL) *versus* 8 % (CONTIN/LL)). A similar difference was observed for Aβ(1-42) (26 % (CDANAL) *versus* 8 % (CONTIN/LL)). These

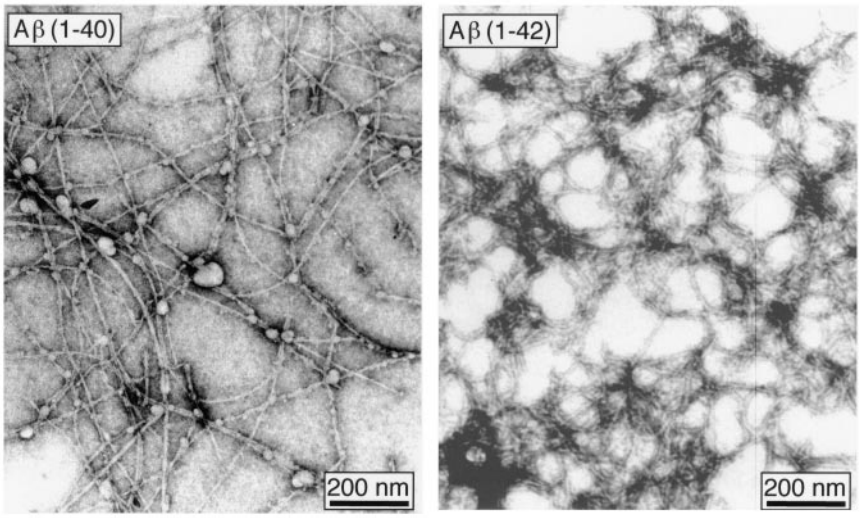

Figure 2. Morphology of Aβ assemblies. Aliquots of the Aβ(1-40) and Aβ(1-42) samples on which CD experiments were performed (Figure 1) were removed for negative staining and transmission electron microscopy (EM). In each case, twisted fibrils of ~8 nm diameter and indeterminate length were observed. These results are representative of those obtained in each of seven independent experiments. Scale bars represent 200 nm.

differences in β-turn levels were accompanied by compensatory differences in RC content. Thus the sums of the β-turn and random-coil components of each peptide were similar for each deconvolution method, differing by ~7% for Aβ(1-40) and ~4% for Aβ(1-42). Taken together, these data are consistent with a process in which Aβ coil and turn regions rearrange to give rise to α-helices and β-sheets.

We next used CD to examine the time-dependent conformational changes occurring during fibrillogenesis of the 16 different Aβ alloforms.

Table 2. Characteristics of helix formation by Aβ alloforms

Peptide	α_{max} (%)	t_{max} (days)
Aβ(1-42)	19	4
[Gly21]Aβ(1-42) (Flemish)	24	5
[Gly22]Aβ(1-42) (Arctic)	20	5
[Gln22]Aβ(1-42) (Dutch)	21	3
[Lys22]Aβ(1-42) (Italian)	22	4
Aβ(3-42)	22	5
[< E^{3}]Aβ(3-42)	23	4
Aβ(11-42)	23	4
[< E^{11}]Aβ(11-42)	22	13
Aβ(1-40)	32	12
[Gly21]Aβ(1-40) (Flemish)	27	10
[Gly22]Aβ(1-40) (Arctic)	26	8
[Gln22]Aβ(1-40) (Dutch)	32	4
[Lys22]Aβ(1-40) (Italian)	27	11
Aβ(3-40)	31	11
[< E^{3}]Aβ(3-40)	30	15
Aβ(11-40)	28	9
[< E^{11}]Aβ(11-40)	25	17

CD spectra were acquired daily for 21 days during fibrillogenesis of peptides at pH 7.5. Spectral deconvolution and comparison revealed the day (t_{max}) at which maximal helix content was observed and the percent helix content on that day (α_{max}). Helix percentages are rounded to the nearest integer.

Without exception, each of these peptides exhibited time-dependent conformational changes similar to those observed for Aβ(1-40) and Aβ(1-42). The t_{max} and α_{max} values for these alloforms are listed in Table 2. The kinetics of formation of the α-helix-containing intermediate correlates with the kinetics of fibrillogenesis. It is not until helix formation has begun that fibrils are detected by EM. For example, helix content in Aβ(1-40) begins to rise following approximately three days of incubation, whereas short fibrils are not observed until day 6 (Figure 1(b)). For Aβ(1-42), helix content rises immediately following peptide dissolution and approaches α_{max} at the time fibrils are first observed (day 3). Because each Aβ monomer does not fold and assemble synchronously with every other monomer, a distribution of conformational/assembly states exists prior to the completion of the fibrillogenesis process. This explains why unstructured Aβ monomers, helix-containing oligomers, and fibrils coexist at some stages of fibril assembly. At the end of the process, when α-helix content had decreased to negligible levels, dense fibril aggregates were observed for both peptides.

The structural diversity of the 18 peptides studied allowed observations to be made regarding the effects of clinically relevant truncations, amino acid residue substitutions, and N-terminal pyroglutamylation on fibrillogenesis kinetics (Table 2). The most significant effect on t_{max} and α_{max} was mediated by the dipeptide Ile41-Ala42 (numbering relative to Aβ(1-42)). For each of the nine pairs of Aβ alloforms in which the only structural difference was the presence or absence of Ile41-Ala42, the peptide containing Ile41-Ala42 displayed both a reduced t_{max} and a reduced α_{max}. It therefore appears that the primary kinetic effect of deletion of Ile41-Ala42 is to retard fibrillogenesis, regardless

of the length or sequence of the Aβ alloform from which the dipeptide was removed. N-terminal truncation had little effect on fibrillogenesis kinetics, with the exception that Aβ(11-40) showed a modest decrease in t_{max} relative to wild-type Aβ(1-40). In contrast, cyclization of N-terminal Glu to form pyroglutamyl (<E) peptides retarded the rate of helix formation of Aβ(11-40), as well as that of Aβ(3-40) and Aβ(11-42). This modification had little effect on Aβ(3-42). The combination of pyroglutamylation and deletion of Ile41-Ala42, as found in [< E^3]Aβ(3-40) and [< E^{11}]Aβ(11-40), produced the greatest retardation of fibrillization rate (t_{max}) observed among the 18 peptides.

In addition to Aβ peptide truncation and N-terminal cyclization, which appear to occur *in vivo* in Aβ deposition diseases, a cluster of amino acid residue substitutions has been discovered involving Ala21 and Glu22. These substitutions are associated with familial amyloidoses in which extensive cerebrovascular amyloid deposition occurs. Based on the ethnicity of the kindreds in which they were discovered, the substitutions have been termed Flemish (Ala21 → Gly),[49] Arctic (Glu22 → Gly),[50] Dutch (Glu22 → Gln),[51] and Italian (Glu22 → Lys).[52] In Aβ(1-40), these substitutions increased the rate of α-helix formation relative to their wild-type homologues (Table 2). Little effect was observed when the substitutions were made in Aβ(1-42). However, the Dutch variant, [Gln22]Aβ(1-42), displayed the smallest t_{max} (3d) of any of the nine peptides containing Ile41-Ala42, and [Gln22]Aβ(1-40) had the smallest t_{max} (4d) of any of the nine peptides missing Ile41-Ala42. In fact, [Gln22]Aβ(1-40) proceeded to α-helix formation at a rate equal to that of wild-type Aβ(1-42), but α_{max} of [Gln22]Aβ(1-40) was as high as that of wild-type Aβ(1-40). Taken together, the above studies show that the formation of a partially helical intermediate is a general feature of Aβ fibrillogenesis and that the levels of helix observed and the kinetics of helix formation are affected by specific alterations in peptide length and sequence.

Assembly state of the α-helical intermediate

Recent studies of a model folding intermediate, αtα, have shown that oligomeric assemblies of helical monomers may form prior to β-sheet and fibril formation.[53] In an effort to characterize the structure(s) of the Aβ α-helix-containing-intermediates, CD experiments were performed on wild-type Aβ(1-40) before and after its fractionation by filtration. To do so, low molecular weight (LMW) Aβ was incubated at a concentration of 25 μM in 10 mM glycine buffer (pH 7.5), at 22 °C until maximal α-helix was observed. This typically occurred after 11-12 days. At this point, the sample was filtered through a 10k MWCO Centricon filter and the filtrates and retentates were analyzed by CD (Figure 3) and amino acid analysis (Table 3). The majority (>90 %) of Aβ was non-filterable, thus the assemblies in this fraction had minimal molecular mass >10,000, consistent with the presence of trimers and higher-order oligomers and polymers. Analysis of CD spectra collected on three independent samples of the retentate showed the presence of conformers containing 29-32 % α-helix (Figure 3). The α-helix content in each of these samples was

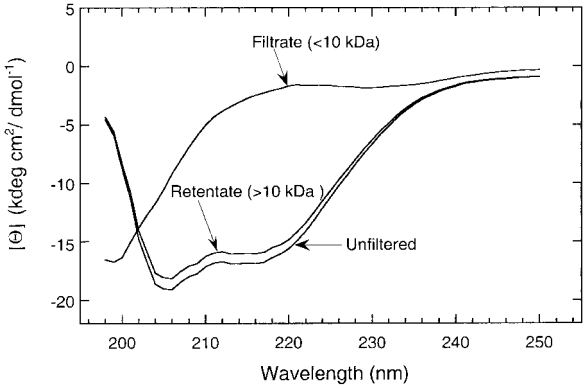

Figure 3. Size characterization of α-helix-containing intermediates. Aβ(1-40) was dissolved at a concentration of 25-30 μM in 10 mM glycine buffer (pH 7.5), filtered using 10k MWCO membranes, and incubated at 22 °C until α_{max} was observed (typically after 11-12 days). The sample then was filtered through a 10k filter and spectra acquired both from the material passing through the membrane (filtrate) and the material retained by the membrane (retentate). CD spectra are presented of the untreated sample and the two fractions resulting from filtration. These results are representative of those obtained in each of three independent experiments.

Table 3. Assembly state of the α-helix-containing intermediate

MWCO	Filtrate (%)	Retentate (%)	Loss (%)
10	9 ± 1	65 ± 3	26 ± 2
30	9 ± 2	63 ± 2	27 ± 2
50	10 ± 1	63 ± 1	27 ± 2
100	9 ± 2	64 ± 1	27 ± 4

LMW Aβ(1-40) was incubated in 10 mM glycine buffer (pH 7.5), at 22 °C for 11-12 days. Samples then were filtered through 10k, 30k, 50k, or 100k Centricon filters and the peptide concentrations in the filtrates and retentates determined by AAA. Recovery (%) was determined relative to the starting peptide mass prior to filtration. The difference between starting peptide mass and the sum of filtrate and retentate masses is considered ''loss.'' This loss likely results from peptide adsorption to surfaces. The apparent lack of mass conservation in the 30k experiment is due to rounding errors.

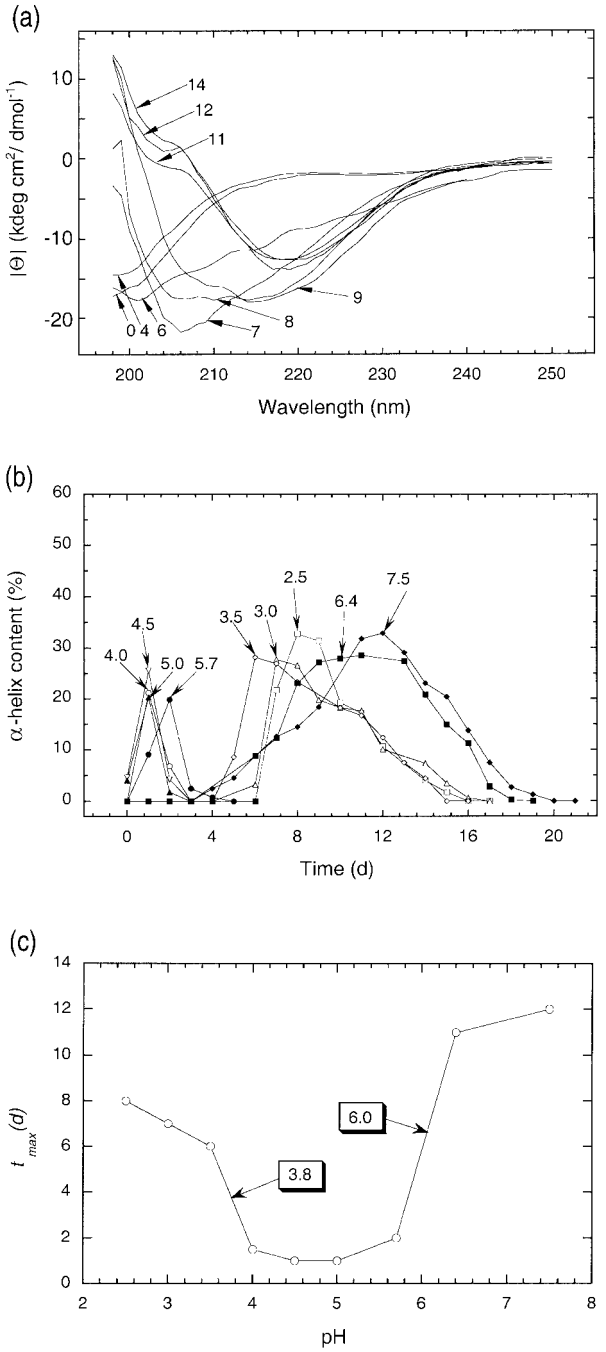

Figure 4. pH dependence of the kinetics of formation of α-helix-containing intermediates. (a) Aβ(1-40) was dissolved at a concentration 25-30 μM in 10 mM glycine buffer (pH 3.0), filtered through a 10k MWCO membrane, incubated at 22 °C, and monitored daily by CD. The spectra demonstrate a transition from RC to β-sheet through a transitory α-helix-containing intermediate. Results are expressed as molar ellipticity [Θ] (kdeg cm^2 dmol^{-1}). The spectra shown are averages of three scans each with an averaging time five seconds. These results are representative of those obtained in each of three independent experiments. (b) Aβ(1-40) was studied as detailed above, except over a pH range of 2.5-7.5. The amounts of α-helix are plotted *versus* time in days (d). These results are representative of those obtained in each of three independent experiments. (c) t_{max}, the time at which maximal α-helix content was observed, is plotted against pH. The curve resembles a trough in which helices form fastest at its center (pH 4-5.7) and slowest at its edges. The kinetics of helix formation was faster at low pH than at high pH and displayed steep transitions centered at ~pH 3.8 and ~pH 6.0.

identical with that of the unfiltered material. In contrast, the filterable material, nominally monomeric or dimeric, produced CD spectra characteristic of LMW Aβ. To further estimate the size of the intermediate, the filtration experiment was repeated using 30k, 50k, and 100k MWCO devices. The results were essentially identical with those obtained using 10k filters. In each case, >90 % of the peptide mass was non-filterable, and it was this population of Aβ peptides that contained the α-helix-rich conformers (Table 3). Based on a spherical geometry, these results are consistent with the existence of an α-helix-containing assembly intermediate containing a minimum of 23 Aβ monomers. It should be noted that the apparent hydrodynamic radius of an Aβ oligomer could increase substantially if it were non-spherical.[54] In this case, the number of monomers composing the oligomer would be proportionately lower.

pH-dependence of α-helix formation kinetics

As a first step towards understanding the mechanistic basis for the formation of helix-containing intermediates, studies were done to determine the pH dependence of the phenomenon. Temporal changes in the α-helix content of Aβ(1-40) conformers were determined over the pH range 2.5-7.5 during incubation of the LMW peptide at a concentration of 25 μM in 10 mM glycine buffer at 22 °C. Figure 4(a) shows the CD spectra collected during incubation at pH 3.0 and is illustrative of the secondary-structure changes observed during incubation at each pH value. Here, a clear conformational transition from random coil (day 0) → α-helix-containing intermediate (day 8) → β-strand (day 14) is apparent. Figure 4(b) presents the temporal changes in α-helix content observed at each pH value. At the lowest pH, 2.5, α-helix content remains negligible through day 6, after which a rapid rise occurs, producing an α_{max} of 30 % on day 8. Following this maximum, a relatively slow decline in helix content occurs until no helix is observed. Similar time-dependent changes in helix content were seen at pH 3.0 and 3.5, except that helix formation was detected earlier and the α_{max} values were lower. t_{max} occurred earliest in the pH range 4.0-5.7. In this range, the rise and fall in helix content occurred over a period of two to three days and produced an almost symmetric curve. In addition, α_{max} was the lowest in this pH regime, ranging from ~20 to 26 %. Above pH 4.5, a direct correlation between pH and α_{max} or t_{max} was seen. At pH 5.7, t_{max} occurred at day 2, one day later than observed at pH 4.0-5.0. Increasing the

pH to 6.4 or 7.5 shifted t_{max} to day 11 and day 12, respectively, longer than observed at the lowest pH conditions, and produced curves characterized by the relatively early appearance of helix (day 5) and a slow rise and fall in helix content. A trend toward lower helix levels in samples studied at pH 4.0-5.7 likely results from the rapid fibrillogenesis kinetics observed in this pH regime, which would minimize accumulation of the metastable helix-containing oligomer.

Conceptional insights into the mechanism(s) controlling the kinetics of formation of the α-helix-containing intermediate were achieved by studying the relationships of t_{max} to pH (Figure 4(c)). The curve produced by the data resembled a trough. Helices formed fastest in the pH range 4.0-5.7, the bottom of the trough. At the extremes of pH, the edges of the trough, the kinetics of helix formation were faster at low pH values than at high pH values. The walls of the trough represent two distinct transitional zones. The first occurred between pH 3.5 and 4.0, with a midpoint at pH 3.8, and the second occurred between pH 5.7 and 6.4, with a midpoint at pH 6.0. Within experimental error, these midpoint pH values are identical with those of aspartic acid (3.86) and histidine (6.0).[55] The most rapid formation of the partially helical intermediate thus occurs in the pH regime in which the β-carboxyl group of Asp is ionized and the imidazole ring of His is protonated.

Mechanisms controlling α-helix formation

To test the hypothesis that aspartic acid or histidine residues might control the kinetics of α-helix formation, and therefore of fibrillogenesis, a series of eight modified Aβ peptides were synthesized in which Asp or His were replaced by Asn and Gln, respectively, either singly or in various combinations (Table 1). The pH dependence of the kinetics of α-helix and fibril formation was then studied using CD. Asn and Gln were chosen based on chemical and genetic grounds. Asn is similar in size to Asp and does not ionize, thus it provides a means of evaluating the role of the β-carboxyl group in controlling the fibrillogenesis process. A similar rationale was employed in substituting Gln for His. In addition, mutation data matrices,[56] which provide estimates within protein families of the probability that a given amino acid residue in a protein will be substituted by a given second amino acid residue, show that protein evolution favors Asp → Asn and His → Gln substitutions, presumably because they conserve the functional capabilities of the wild-type protein.

Modified peptides were synthesized both on Aβ(1-40) and Aβ(1-42) ''backgrounds.'' However, modified Aβ(1-42) peptides were poorly soluble, resulting in poor-quality CD spectra. Experiments were thus restricted to the Aβ(1-40) peptides. Wild-type Aβ(1-40) and each of the modified peptides were incubated at 22 °C in 10 mM glycine buffer at pH 3.0, 3.5, 4.0, 5.0, 5.7, and 7.5, and their CD spectra were acquired daily for 17-21 days. t_{max} values were then determined. The pH conditions were chosen to encompass the pK values for Asp and His. No significant differences in the rates of helix formation were observed among any of the peptides tested at pH 3.0, 3.5 and 7.5 (Figure 5(a) and (b)), regimes in which only one of the two wild-type amino acid residues are charged. However, in the pH range 4.0-5.7, the Asn23 substitution consistently and significantly delayed helix formation relative to wild-type Aβ. The Asn7 substitution had a similar, and significant, effect at pH 4 and 5, but displayed a statistically insignifi-

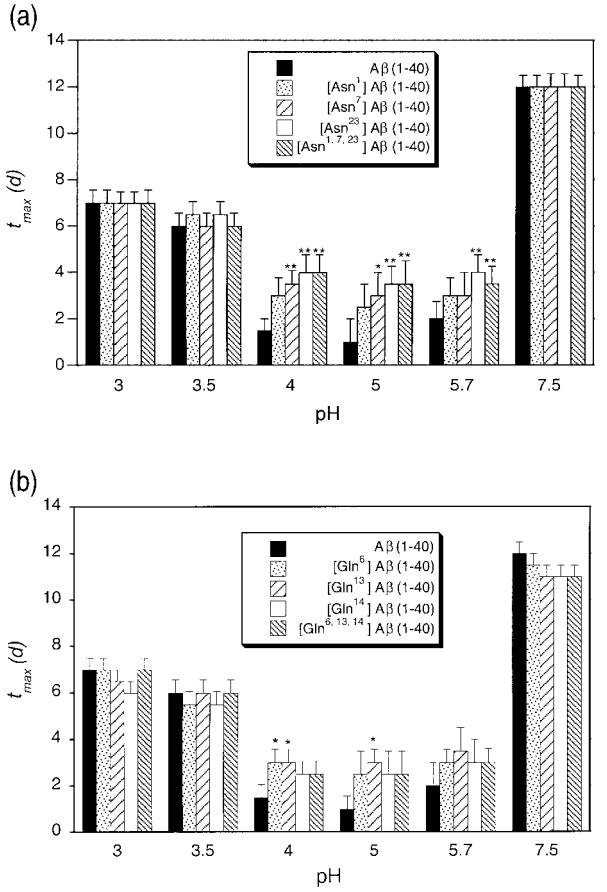

Figure 5. Effects of amino acid residue substitutions on helix formation. (a) Asp → Asn substitutions. Wild-type Aβ(1-40) and singly and triply substituted peptides at 25 μM concentration were incubated at 22 °C in 10 mM glycine buffer, pH values 3.0, 3.5, 4.0, 5.0, 5.7, and 7.5. CD spectra were acquired daily, deconvoluted, and then t_{max} was plotted against pH. For each pH, the statistical significance of differences between t_{max} values of wild-type and modified peptides was determined using a Tukey test (Statview, v5.0.1, SAS Institute Inc., Cary, NC). Significance is indicated as follows: no symbol, not significant; *, $p < 0.04$; **, $p < 0.02$. (b) His → Gln substitutions. Wild-type Aβ(1-40) and singly and triply substituted peptides were studied as above. These results are representative of those obtained in each of four independent experiments.

cant delay at pH 5.7. The Asn1 substitution had no significant effect at any pH. The triply substituted Asn1, 7, 23 peptide behaved similarly to the Asn23 peptide. Based on the behavior of the singly substituted homologues, the primary effector of the altered kinetics observed in the Asn1, 7, 23 peptide is the Asn23 substitution. At pH 4.0-5.7, the Gln-substituted peptides all trended towards delayed helix formation, however significant decreases were observed only at pH 4.0 for the Gln6 and Gln13 peptides and at pH 5.0 for the Gln13 peptide. The Gln13 peptide consistently produced the largest t_{max} at each pH in the range 4.0-5.7. Comparison of the results obtained for wild-type Aβ(1-40) with those from the modified peptides suggest, in particular, that Asp23 and His13 exert significant control over the kinetics of Aβ fibrillogenesis and that the kinetics are most rapid in the pH regime in which the β-carboxyl group of Asp is ionized and the imidazole ring of His is protonated.

Discussion

The amyloidotic neuropathology of AD has been known for almost a century.[57] Following the protein chemical characterization of amyloid deposits[16,58] and the subsequent cloning of the AβPP gene,[33,59–61] intense efforts have been directed towards understanding Aβ metabolism.[4] A key goal of these studies has been to understand fibril assembly in order to develop inhibitory therapeutic agents. Recently, however, compelling evidence has emerged that oligomeric Aβ assemblies may be as damaging to neurons as are fibrils,[10–13] and in fact, that these soluble species may be the primary effectors of neurodegeneration *in vivo*.[62–66] It is thus important that a rigorous mechanistic understanding of the conformational and associative events in Aβ assembly be achieved, both with respect to late stages of fibril formation and to earlier stages leading to oligomer formation.

Here, the conformational transformations of Aβ during its oligomerization and assembly into fibrils have been examined. We find that one of the most prominent early features of fibril assembly is the formation of oligomeric intermediates containing significant amounts of α-helix (up to 32%). A systematic study of the temporal changes in secondary structure among Aβ(1-40), Aβ(1-42), and 16 different biologically relevant Aβ alloforms reveals, without exception, that this helix-containing intermediate is detected prior to the appearance of fibrils and disappears as exponential growth of fibrils proceeds. The pH dependence of the kinetics of helix formation and fibril growth suggests that aspartic acid and histidine residues exert significant control over the process. Direct testing of this hypothesis, done by studying the kinetics of fibrillogenesis of Aβ(1-40) alloforms in which Asp → Asn or His → Gln substitutions were made individually or *en masse*, demonstrated that elimination of certain of the Asp β-carboxylate anions or the His imidazole cations significantly retarded fibrillogenesis.

Helix formation and oligomerization

Our initial studies of the temporal changes in secondary structure of wild-type Aβ were prompted by the observation that a transitory rise in peptide α-helix content occurred during fibrillogenesis of Aβ(1-40)[12] and by an earlier suggestion that helix formation was actually ''off-pathway'' for fibrillogenesis.[27] The results reported here support the hypothesis that, in the initial stages of fibril formation, monomeric Aβ displaying predominately RC secondary structure undergoes a conformational transition to form α-helices and that helix formation is ''on-pathway'' for fibrillogenesis. Filtration studies revealed that the assemblies producing the helix-rich spectra had molecular masses >100,000, demonstrating that the α-helix conversion occurs concurrently with the oligomerization of Aβ. It is interesting that in insulin fibrillogenesis predominately helical peptide monomers oligomerize in the initial stages of the process.[67,68] It is from these intermediates that β-sheet-rich fibrils then emanate. Recent studies of the fibrillogenesis of a model 38-residue helix-turn-helix peptide, αtα, revealed an identical process.[53] Conversion of helix-rich, oligomeric proteins into fibrils has also been observed *in vivo*. For example, in the silk gland of the silkworm, *Samia cynthia ricini*, prior to its extrusion, the silk is helical, whereas during extrusion the protein undergoes a conformational change producing the archetypal cross-β structure.[69] Especially intriguing is the recent observation that Aβ aggregates in diffuse plaques of apolipoprotein E knockout mice[70,71] exist in the form of trabecular networks strikingly similar in morphology to that of the helical glandular silk (R. Brendza, D. Holtzman, and J. Heuser, personal communication). If diffuse plaques are precursors to senile plaques, as some evidence suggests,[72,73] then this observation is consistent with a mechanism in which oligomeric, helix-rich assemblies in these deposits convert to fibrils.

Our data, and those of others cited above, are consistent with a fibrillogenesis process involving helix-containing intermediates; however, other interpretations are also possible. For example, although helix and fibril formation are correlated temporally, a ''cause and effect'' relationship may not exist. This would be the case if the helix-containing oligomer were a metastable peptide ''sink,'' incapable of maturing into fibrils. In order to produce the time-dependent changes in secondary structure and peptide-assembly state observed here, these sinks would be in rapid equilibrium with smaller Aβ oligomers or with Aβ monomers, species which could form fibrils through an alternative pathway. In addition, conditions facilitating helix formation should decrease the energy barrier for formation of the helix-containing

intermediate and result in an inhibition of fibrillogenesis.

The debate about whether formation of helix-containing oligomers are ''on'' or ''off'' the pathway of fibril formation may be more apparent than real. An increasing body of evidence suggests that not only Aβ fibrillogenesis, but also the fibrillogenesis of a number of other peptides and proteins, involves the formation of oligomeric assemblies.[74–78] The evidence presented here supports a conformational model in which helix → strand transitions in these oligomers lead to fibril formation. If so, structural changes in the Aβ peptide which stabilize helical structure would have the potential to inhibit fibril formation, as reported by Soto *et al*.[27] In fact, the addition of moderate to high concentrations of the helix-premissive fluorinated alcohol trifluroethanol (TFE) to solutions of Aβ can indeed facilitate helix formation yet prevent fibril formation (Y. Fezoui and D.B.T., unpublished results). This observation is also consistent with the alternative hypothesis that the oligomeric intermediate is off-pathway, because if the intermediate is a peptide sink, then the transiting of Aβ into this conformational space would prevent fibril assembly. However, by this logic, any facilitation of helix formation should inhibit fibrillogenesis, at least to some degree. Experimentally, this is not the case. In fact, at TFE levels up to ~20 %, a concentration-dependent acceleration of fibril formation recently has been observed (Y. Fezoui and D.B.T., unpublished results). Based on simple thermodynamic grounds, these observations are not surprising. Amino acid residue substitutions or solvent conditions which lower the energy barrier for helix formation will facilitate fibril formation if, at the same time, the energy barrier for conversion of the helix-containing intermediates to fibrils is not increased significantly. This situation exists at low TFE concentration. However, conditions which create a deep energy well for the helical state, as occurs at higher TFE concentration or with an [Ala18]Aβ(1-40) alloform,[27] will trap Aβ in this conformational space and prevent fibril formation.

Systematic comparison of primary structure effects on fibrillogenesis kinetics

An additional benefit arising from the experiments studying the generality of fibrillogenesis-related helix formation was the ability to compare the fibrillogenesis kinetics of many of the most important biologically relevant alloforms of Aβ. This comparison allowed the evaluation of the relative importance of particular primary-structure elements in controlling fibril formation. We found that the primary determinant of fibrillogenesis rate was the presence or absence of Ile41-Ala42. Peptides containing these two residues always formed fibrils faster than did their homologues lacking these residues, regardless of the primary structures involved. For eight of nine peptides containing Ile41-Ala42, t_{max} occurred between three and five days. By comparison, peptides ending at the equivalent of Val40 displayed t_{max} values ranging up to 17 days. The only Ile41-Ala42-containing peptide whose fibrillogenesis rate was retarded relative to wild-type Aβ(1-42) was [< E^{11}]Aβ(11-42). In fact, next to the effect of Ile41-Ala42, the most significant changes in fibrillogenesis kinetics were produced by N-terminal pyroglutamylation, which always slowed the rate of fibrillogenesis. This was true not only for [< E^{11}]Aβ(11-42), but for [< E^{11}]Aβ(11-40) and [< E^{3}]Aβ(3-40) as well. The powerful kinetic effect of the Ile41-Ala42 dipeptide suggests that its presence is required for the formation of a thermodynamically stable structural unit within the Aβ fibril.

The presence of Ile41-Ala42 accelerated fibrillogenesis, regardless of the structure of the remaining N-terminal portion of the peptide. However, in the cases of [< E^{11}]Aβ(11-42) and [< E^{11}]Aβ(11-40), the fibrillogenesis rate of each peptide was the slowest among the eight different peptides with which it shared the same C terminus. This finding was curious because [< E^{11}]Aβ(11-42) is present in large amounts in both insoluble and soluble fractions of AD brain.[79–81] Why would this be if its structure so significantly retarded its fibrillogenesis? One explanation is that amyloid deposition is a function both of the intrinsic propensity of each peptide to assemble and of the body's capacity to catabolize the peptide. Thus, during an extended disease process such as that occurring in AD, peptides which form stable assemblies will tend to accumulate, even if their relative concentrations in the brain are low. In fact, Russo *et al*.[82] have shown in primary cultures of rat astrocytes that synthetic [< E^{3}]Aβ(3-40), [< E^{3}]Aβ(3-42) and [< E^{11}]Aβ(11-42) are more resistant to degradation than are Aβ(1-40) or Aβ(1-42). This mechanism may also operate in the Flemish variant of AD,[49] for which *in vitro* studies have shown that the Ala21 → Gly substitution actually slows fibrillogenesis relative to wild-type Aβ.[83]

Among the peptides associated with familial forms of amyloidosis, the Dutch peptides fibrillized significantly more rapidly than did the others, or did wild-type Aβ, as reported.[51,84–86] Accelerated assembly kinetics were also observed with the Arctic Aβ(1-40) alloform. This observation is intriguing in light of the fact that the Arctic substitution has been shown to increase the rate of formation, and the stability, of protofibrillar intermediates.[87] Consistent with this observation, electron-microscopic examination of peptide assemblies formed by the Arctic peptide revealed fewer mature fibrils than did other Aβ species incubated under equivalent conditions (data not shown). Both the Flemish and the Italian Aβ(1-40) alloforms displayed fibrillogenesis kinetics which were similar to those of wild-type Aβ(1-40). However, the Italian peptides assembled into fibrils which were shorter and more branched than those from wild-type peptides. Miravalle *et al*.[86] have also reported that the Italian substitution results in shorter fibrils. In

addition, they suggest that the charge state of the amino acid is a factor in the cytotoxic effects and vascular localization of the resulting amyloid.

Roles of Asp and His in controlling fibrillogenesis kinetics

Therapeutic strategies which seek to prevent the RC or β-turn → α-helix or α-helix → β-strand transitions require targets. As a first step towards determining which amino acid residues are important in controlling the kinetics of helix formation, the pH dependence of the kinetics was examined. The results showed that the most rapid kinetics occur in the pH range 4-5.5 and that the kinetics exhibit two sharp transitional zones which were coincident with the pK values of Asp and His. Interestingly, chemical-shift changes observed in NMR studies of Aβ fibrillogenesis at neutral pH suggest that residue-specific interactions involving Asp and His occur early in the process (M. Zagorski, personal communication).

Our spectroscopic data are consistent with earlier data suggesting that Asp and His play important roles in Aβ fibril production and stability. For example, it has been found that imidazole-carboxylate salt bridges between the side-chains of aspartic acid and histidine residues are critical to the formation of the amyloid β-sheet structures.[32,88–90] In addition, His residues appear to be recognition sites for proteins such as transthyretin and for zinc cations, which can prevent or promote aggregation.[91,92] More significantly, disruption of these salt bridges promotes fibril dissolution.[93] Comparing the kinetics at the extremes of pH measured, we found that fibrillogenesis proceeded more rapidly at acidic pH than at neutral or basic pH. This is consistent with a significant influence of the central hydrophobic cluster (CHC) of amino acid residues, Leu17-Ala21, on fibrillogenesis kinetics.[94] Evidence exists that one of the initial steps in Aβ folding is the hydrophobic ''collapse'' of this region into a compact structure.[26,88] At low pH, both Glu22 and Asp23 are uncharged, which would produce a decrease in electrostatic potential in the CHC and cause an enhancement of interactions between uncharged side-chains.[84]

We addressed directly the hypothesis that Asp and His exerted significant control over fibrillogenesis kinetics by synthesizing a series of Aβ(1-40) peptides containing single and multiple Asp → Asn and His → Gln substitutions and then studying the pH dependence of the rate of formation of the helix-containing intermediate. The results showed that the Asp23 anion and the His13 cation were particularly important in facilitating formation of the intermediate, as the elimination of these charges significantly inhibited the process. It should be noted that the Asp → Asn and His → Gln substitutions change the pI values of the resulting singly substituted peptides from ~5.5 to 6.2 and 4.8, respectively. Because protein solubility and aggregation propensity can change dramatically near the pI, it was possible that the changes in kinetics we observed were due simply to a pI effect. However, the experiments revealed no obvious shifts in the pH dependence of the fibrillogenesis kinetics, suggesting that the effects we observed were residue specific. In fact, although the pI of the triply-substituted Asp → Asn alloform is 2.3 units higher than that of wild-type Aβ (7.8 *versus* 5.5), the peptide behaved similarly to the singly substituted Asp23 → Asn alloform.

As discussed above, early studies of fibril formation by Aβ peptide fragments terminating at Lys28,[89] and by the fragment Aβ(11-25),[90] have suggested that Asp23 and His13 may function in the formation of salt-bridges. In addition, these studies suggested that His13 might be involved in intersheet packing interactions. This idea is supported by recent results demonstrating that a His13 → Ala substitution in Aβ(1-28) dramatically inhibits fibril formation and alters fibril morphology.[95] We demonstrate here that His13 is also important in the fibrillization of the biologically relevant full-length form of Aβ, both with respect to the RC or β-turn → α-helix transitions involved in formation of fibril intermediates and with respect to the subsequent α-helix → β-strand conversion associated with transformation of the intermediates into fibrils.

The issue of biological relevance is not trivial. Although many model peptides have been used to examine biophysical and physiological aspects of Aβ peptide behavior,[22] not all peptides are satisfactory proxies for the forms of Aβ found *in vivo*. For example, studies of the effects of isomerization of Asp23 on fibrillogenesis kinetics have revealed both the importance of this residue in controlling fibrillogenesis and the necessity of evaluating the functional effects of peptide primary structure using the biologically relevant peptides.[96,97] This latter point arose from the observation that racemization of Asp23 in Aβ(1-35), a nominal model for [D-Asp23]Aβ(1-40), accelerated peptide aggregation, whereas in the biologically relevant full-length peptide, Asp23 racemization retarded fibrillogenesis. Retardation of fibril formation also has been reported in studies of the singly substituted Aβ alloform [Lys23]Aβ(11-25).[90] In contrast, isomerization of Asp23 in Aβ(1-42) recently was shown to result in increased production of Thioflavin T positive assemblies.[98] We find that an Asp23 → Asn substitution retards fibrillogenesis. Taken together, these data emphasize the importance of Asp23 in controlling Aβ folding and assembly.

Asp23→Asn, a convergence of basic and clinical research

Our basic studies of Aβ folding and assembly led to the hypothesis that Asp23 plays a key role in the fibrillogenesis process. To test this hypothesis, fundamental chemical and genetic principles

were used to design an altered peptide, containing Asn23, whose fibrillogenesis behavior was predicted, and found, to differ from that of wild-type Aβ. In particular, the kinetics of fibril formation and the morphology of the resulting fibrils were distinct. However, what could not be predicted, and what has produced an unexpected *in vivo* confirmation of the predictions of our model, is the recent discovery of a kindred in Iowa in which a mutation in AβPP produces an Asp23 → Asn substitution in Aβ, resulting in a particularly aggressive form of CAA.[99] The disease caused by this ''Iowa mutation'' is characterized by an early onset, severe vascular amyloid deposition and vessel damage, formation of ''cotton wool'' plaques in the neuropil, widespread neurofibrillary tangle formation, and white matter pathology.[99] In addition, the Iowa peptide has been found to be toxic to cultured human vascular smooth muscle cells (W. Van Nostrand, personal communication). It thus appears that structural changes involving Asp23 can produce peptides and/or peptide assemblies that damage the vascular endothelium both through direct physiological insult and mechanical means. The kinetic studies presented here suggest that the latter mechanism results from increased stability of the peptide assemblies, which inhibits their catabolism.

α-helix→β-strand transitions and Aβ fibrillogenesis

The *in vitro* studies presented here are consistent with a model of Aβ fibrillogenesis in which an oligomeric intermediate composed of partially helical Aβ monomers gives rise to amyloid fibrils. This intermediate may exhibit up to one-third helical character, but following fibril formation, no helix component is observed in the system. Rather, the predominant secondary-structure elements are β-strand (~50 %), β-turn (~20 %), and RC (~20 %). Both RC → β-strand and α-helix → β-strand conversions may contribute to the formation of the extended β-sheet within the fibril core. In the case of Aβ(1-40), it is the helix → strand transition which appears to provide the bulk of nascent β-strand. In fact, recent IR studies of temperature-induced aggregation of Aβ(1-40) in the solid state have shown directly that a significant α-helix → β-structure conversion occurs.[100] *In vivo*, it is likely that the Aβ region of AβPP exhibits substantial helical character due to its association with, and partial constitution of, the AβPP transmembrane domain. The exact level of α-helix is unknown, however, if all 14 C-terminal amino acid residues of Aβ, i.e. Gly29-Val42, maintained their helical state following γ-secretase-mediated release of the peptide from AβPP, then the level would be one-third. Fibril formation from these nascent Aβ conformers thus would involve an extensive α-helix → β-strand conversion process. α-helix → β-strand transitions occur during the normal folding of proteins such as lysozyme[101] and β-lactoglobulin,[102] and during amyloid fibril formation by prion protein[103] and insulin.[67] *In vitro* studies have shown that model helical peptides can be constructed which fold into β-sheets and form fibrils.[53,104] These peptide models have facilitated the experimental identification of important structural factors controlling the α-helix → β-strand transition.[105]

A recent study by Kallberg *et al.*[106] suggests that fibril formation mediated through α-helix → β-strand transitions may be more frequent than has been realized. Here, secondary-structure predictions were made for 1324 non-redundant proteins. In 37 cases, β-strands of seven residues were predicted in peptide segments which were known experimentally to exist as helices. This ''discordance'' was observed in a number of amyloidogenic proteins, including prion protein and Aβ, suggesting that the discordance was predictive of amyloid-forming propensity. In fact, direct experimental study of a number of these helix-containing proteins revealed for the first time that they could, indeed, form typical β-sheet-containing fibrils. In the future, it is likely that many additional examples of alternative protein folding pathways leading to amyloid fibril assembly will be discovered. Rigorous examination of the biophysical and thermodynamic bases for pathway ''choice'' should improve both our basic understanding of protein folding and our ability to develop rational approaches for treating diseases resulting from aberrant protein assembly.

Materials and Methods

Chemicals and reagents

Chemicals were obtained from Sigma and were of the highest purity available. Water was double distilled and deionized using a Milli-Q system (Millipore Corp., Bedford, MA).

Peptide synthesis

Aβ peptide synthesis, purification, and characterization have been described.[75,107] Briefly, Aβ(1-40), Aβ(1-42), and 24 different peptide alloforms (Table 1) were made on an automated peptide synthesizer (Model 430A, Applied Biosystems, Foster City, CA) using 9-fluorenylmethoxycarbonyl-based methods. Peptides were purified using reversed-phase high-performance liquid chromatography (RP-HPLC). Quantitative amino acid analysis and matrix-assisted laser desorption/ionization time-of-flight mass spectrometry yielded the expected compositions and molecular masses, respectively, for each peptide. In addition, peptides were sequenced (model 477A, Applied Biosystems, Foster City, CA) if any inconsistencies in composition or mass were observed. Purified peptides were stored as lyophilizates at −20 °C. When possible, in order to maximize chemical homogeneity among related peptides, multiple peptides were synthesized from the same starting resin by resin splitting at sites of sequence variation. Aβ(1-40) alloforms were synthesized using preloaded [Val]Wang resin. Aβ(1-42) and its alloforms were made in analogous manner using preloaded [Ala]Wang resin.

Peptide assembly

Peptides were prepared by initial dissolution in distilled water, followed by the addition of glycine buffer, adjusted to an appropriate pH with HCl or NaOH, to yield a final buffer concentration of 10 mM and a final peptide concentration of 25-30 μM. Samples were sonicated for three minutes at 22 °C in an ultrasonic water bath (model B1200-R, Branson Ultrasonics Corp., Danbury, CT), transferred into centrifugal filters (10,000 molecular weight cut off (MWCO), Centricon, YM-10, Millipore Corp., Bedford, MA) and centrifuged at 16,000 *g* using a benchtop microcentrifuge (Eppendorf model 5415 C, Brinkmann Instruments Inc., Westbury, NY) for 20 minutes in order to obtain low molecular weight (LMW) Aβ (monomers or dimers).[12] The filtrate of each sample then was collected and incubated at 22 °C, without agitation, to allow fibril formation to occur. The pH of the sample was checked periodically during the course of each experiment and was found to remain constant throughout.

To examine the effects of primary structure on the conformational transitions and kinetics of fibril assembly, circular dichroism spectroscopy (CD) was performed at pH 7.5 on Aβ(1-40), Aβ(1-42), and their 16 naturally occurring alloforms (Table 1, top 18 peptides). The peptides were prepared essentially as described above, except they were pretreated with dilute sodium hydroxide and relyophilized prior to dissolution.[108] This treatment has been found to significantly improve peptide solubility and decrease *de novo* aggregate formation,[108] factors which were of particular importance for the peptides terminating at Ala42. To study the effects of pH, CD was used to monitor the secondary structure of LMW Aβ(1-40) incubated at 22 °C in 10 mM glycine buffer at pH 2.5, 3.0, 3.5, 4.0, 4.5, 5.0, 5.7, 6.4, and 7.5. To study how single or multiple Asp → Asn and His → Gln substitutions in Aβ (Table 1) affected the kinetics of formation of α-helix-containing intermediates and of fibrils, CD was performed on wild-type and modified Aβ(1-40) peptides incubated in 10 mM glycine buffer at 22 °C at pH 3.0, 3.5, 4.0, 5.0, 5.7, and 7.5.

Circular dichroism spectroscopy (CD)

Samples were prepared for analysis by gently drawing up, and then expelling, the peptide solution into a 200 μl pipette tip. After three cycles, an aliquot was placed into a 0.1 cm pathlength quartz cell (Hellma, Forest Hills, NY) and then CD measurements were performed on an Aviv model 62A DS spectropolarimeter (Aviv Associates, Lakewood, NJ). After spectra were recorded, the aliquot was returned to the original sample tube. Peptide concentrations were 25-30 μM. All measurements were done at 22 °C. Spectra were generally recorded over the wavelength range of 195-240 nm. Extension of the range to lower wavelengths was not possible due to excessive dynode voltages arising from salts present after peptide pretreatment.[108] However, control experiments on untreated peptides showed that deconvolution of spectra extending to 190 nm produced results essentially identical with those from the pretreated samples (data not shown).

Raw data were manipulated by smoothing and subtraction of buffer spectra, according to the manufacturer's instructions. Deconvolution of the resulting spectra was achieved using the program CDANAL[45] and the Brahms and Brahms reference library.[109] The relative amounts of random coil, α-helix, β-sheet and β-turn in each sample were determined from the normalized contribution of each secondary-structure element function to the observed spectrum following curve fitting. In analyses of the temporal changes in secondary structure of Aβ(1-40) and Aβ(1-42), in addition to the application of the CDANAL deconvolution algorithm, a modified version of the CONTIN algorithm, CONTIN/LL, was used.[48,110] In experiments examining fibril formation kinetics, the time (t_{max}) at which α-helix content reached its maximal value was determined by visual inspection of plots of α-helix content *versus* time. The statistical significance of differences between t_{max} values was determined using a Tukey test (Statview, v5.0.1, SAS Institute Inc., Cary, NC). The maximum helix content itself, in percentage terms, is referred to as α_{max}. To determine whether light scattering from large Aβ assemblies might affect the acquisition of the CD spectra, quasielastic light scattering spectroscopy was performed periodically during fibril formation, as described.[54] No significant scattering was observed at the Aβ concentrations used (25-30 μM), whereas at concentrations exceeding 100 μM, substantial scattering was seen (data not shown).

Filtration experiments

To determine the size of helix-rich intermediates, LMW Aβ(1-40) in 10 mM glycine buffer (pH 7.5) was incubated at 22 °C for 11-12 days, the point of maximal α-helix content. CD spectra were then recorded and aliquots of the sample were filtered through 10k, 30k, 50k, or 100k MWCO Centricon filters. The filtrates were collected and analyzed by CD. Retained material (larger than the MWCO) was recovered by gently washing the filter compartment and the top of the filtration membrane with a volume of buffer equal to that of the original aliquot. The resuspended retentates then were analyzed by CD.

Electron microscopy (EM)

Preparation and examination of negatively-stained samples was done essentially as described.[75] Briefly, 10 μl of each sample was applied to a carbon-coated Formvar grid (Electron Microscopy Sciences, Fort Washington, PA), fixed with 10 μl of 0.5 % (v/v) glutaraldehyde, washed gently with distilled water, and stained with 1 % (w/v) uranyl acetate for two minutes. Samples were examined using a JEOL 1200 EX transmission electron microscope.

Acknowledgments

We thank Drs Youcef Fezoui and Gal Bitan for valuable discussions and criticism, Dr Mike Zagorski for sharing with us his unpublished data and his ideas about fibril formation, and Dr Sergei Y. Venyaminov for help with the deconvolution of CD data using CONTIN/LL. This work was supported by grants AG14366 and NS38328 from the National Institutes of Health, and by the Foundation for Neurologic Diseases.

References

1. Iqbal, K. (1991). Prevalence and neurobiology of Alzheimer's disease. In *Alzheimer's Disease: Basic Mechanisms, Diagnosis and Therapeutic Strategies*

(Iqbal, K., McLachlan, D. R. C., Winblad, B. & Winsniewski, H. M., eds), pp. 1-5, John Wiley and Sons, New York.
2. Selkoe, D. J. (1991). The molecular pathology of Alzheimer's disease. *Neuron,* **6**, 487-498.
3. Selkoe, D. J. (1993). Physiological production of the β-amyloid protein and the mechanism of Alzheimer's disease. *Trends Neurosci.* **16**, 403-409.
4. Selkoe, D. J. (1999). Translating cell biology into therapeutic advances in Alzheimer's disease. *Nature,* **399**, A23-A31.
5. Mattson, M. P. (1997). Cellular action of β-amyloid precursor protein and its soluble and fibrillogenic derivatives. *Physiol. Rev.* **77**, 1081-1132.
6. Soto, C. (1999). Alzheimer's and prion disease as disorders of protein conformation: implications for the design of novel therapeutic approaches. *J. Mol. Med.* **77**, 412-418.
7. Schenk, D., Barbour, R., Dunn, W., Gordon, G., Grajeda, H., Guido, T. *et al.* (1999). Immunization with amyloid-β attenuates Alzheimer disease-like pathology in the PDAPP mouse. *Nature,* **400**, 173-177.
8. Janus, C., Pearson, J., McLaurin, J., Mathews, P. M., Jiang, Y., Schmidt, S. D. *et al.* (2000). Aβ peptide immunization reduces behavioural impairment and plaques in a model of Alzheimer's disease. *Nature,* **408**, 979-982.
9. Morgan, D., Diamond, D. M., Gottschall, P. E., Ugen, K. E., Dickey, C., Hardy, J. *et al.* (2000). Aβ peptide vaccination prevents memory loss in an animal model of Alzheimer's disease. *Nature,* **408**, 982-985.
10. Oda, T., Wals, P., Osterburg, H. H., Johnson, S. A., Pasinetti, G. M., Morgan, T. E. *et al.* (1995). Clusterin (ApoJ) alters the aggregation of amyloid β-peptide ($A\beta_{1-42}$) and forms slowly sedimenting Aβ complexes that cause oxidative stress. *Exp. Neurol.* **136**, 22-31.
11. Lambert, M. P., Barlow, A. K., Chromy, B. A., Edwards, C., Freed, R., Liosatos, M. *et al.* (1998). Diffusible, nonfibrillar ligands derived from $A\beta_{1-42}$ are potent central nervous system neurotoxins. *Proc. Natl Acad. Sci. USA,* **95**, 6448-6453.
12. Walsh, D. M., Hartley, D. M., Kusumoto, Y., Fezoui, Y., Condron, M. M., Lomakin, A. *et al.* (1999). Amyloid β-protein fibrillogenesis - Structure and biological activity of protofibrillar intermediates. *J. Biol. Chem.* **274**, 25945-25952.
13. Hartley, D. M., Walsh, D. M., Ye, C. P. P., Diehl, T., Vasquez, S., Vassilev, P. M. *et al.* (1999). Protofibrillar intermediates of amyloid β-protein induce acute electrophysiological changes and progressive neurotoxicity in cortical neurons. *J. Neurosci.* **19**, 8876-8884.
14. Kidd, M. (1964). Alzheimer's disease - an electron microscopical study. *Brain,* **87**, 307-320.
15. Terry, R. D., Gonatas, N. K. & Weiss, M. (1964). Ultrastructural studies in Alzheimer's presenile dementia. *Am. J. Pathol.* **44**, 269-297.
16. Glenner, G. G. & Wong, C. W. (1984). Alzheimer's disease: initial report of the purification and characterization of a novel cerebrovascular amyloid protein. *Biochem. Biophys. Res. Commun.* **120**, 885-890.
17. Glenner, G. G., Eanes, E. D. & Page, D. L. (1972). The relation of the properties of Congo red-stained amyloid fibrils to the β-conformation. *J. Histochem. Cytochem.* **20**, 821-826.
18. Glenner, G. G. (1980). Amyloid deposits and amyloidosis: the β-fibrilloses (second of two parts). *New Eng. J. Med.* **302**, 1333-1343.
19. Glenner, G. G. (1980). Amyloid deposits and amyloidosis. the β-fibrilloses (first of two parts). *New Eng. J. Med.* **302**, 1283-1292.
20. Kirschner, D. A., Abraham, C. & Selkoe, D. J. (1986). X-ray diffraction from intraneuronal paired helical filaments and extraneuronal amyloid fibers in Alzheimer's disease indicates cross-β conformation. *Proc. Natl Acad. Sci. USA,* **83**, 503-507.
21. Tycko, R. (2000). Solid-state NMR as a probe of amyloid fibril structure. *Curr. Opin. Chem. Biol.* **4**, 500-506.
22. Teplow, D. B. (1998). Structural and kinetic features of amyloid β-protein fibrillogenesis. *Amyloid: Int. J. Expt. Clin. Invest.* **5**, 121-142.
23. Rochet, J. C. & Lansbury, P. T., Jr (2000). Amyloid fibrillogenesis: themes and variations. *Curr. Opin. Struct. Biol.* **10**, 60-68.
24. Serpell, L. C. (2000). Alzheimer's amyloid fibrils: structure and assembly. *Biochim. Biophys. Acta,* **1502**, 16-30.
25. Zagorski, M. G., Shao, H., Ma, K., Yang, J., Li, H., Zeng, H. *et al.* (2000). Aβ(1-40) and Aβ(1-42) adopt remarkably stable monomeric and extended structures in water solution at neutral pH. *Neurobiol. Aging,* **21**, S10-S11.
26. Zhang, S., Iwata, K., Lachenmann, M. J., Peng, J. W., Li, S., Stimson, E. R. *et al.* (2000). The Alzheimer's peptide Aβ adopts a collapsed coil structure in water. *J. Struct. Biol.* **130**, 130-141.
27. Soto, C., Castaño, E. M., Frangione, B. & Inestrosa, N. C. (1995). The α-helical to β-strand transition in the amino-terminal fragment of the amyloid β-peptide modulates amyloid formation. *J. Biol. Chem.* **270**, 3063-3067.
28. Sticht, H., Bayer, P., Willbold, D., Dames, S., Hilbich, C., Beyreuther, K. *et al.* (1995). Structure of amyloid A4-(1-40)-peptide of Alzheimer's disease. *Eur. J. Biochem.* **233**, 293-298.
29. Coles, M., Bicknell, W., Watson, A. A., Fairlie, D. P. & Craik, D. J. (1998). Solution structure of amyloid β-peptide(1-40) in a water-micelle environment - is the membrane-spanning domain where we think it is? *Biochemistry,* **37**, 11064-11077.
30. Barrow, C. J., Yasuda, A., Kenny, P. T. M. & Zagorski, M. (1992). Solution conformations and aggregational properties of synthetic amyloid β-peptides of Alzheimer's disease. *J. Mol. Biol.* **225**, 1075-1093.
31. Shao, H. Y., Jao, S. C., Ma, K. & Zagorski, M. G. (1999). Solution structures of micelle-bound amyloid β-(1-40) and β-(1-42) peptides of Alzheimer's disease. *J. Mol. Biol.* **285**, 755-773.
32. Kirschner, D. A., Inouye, Y., Duffy, L. K., Sinclair, A., Lind, M. & Selkoe, D. J. (1987). Synthetic peptide homologous to β-protein from Alzheimer disease forms amyloid-like fibrils *in vitro*. *Proc. Natl Acad. Sci. USA,* **84**, 6953-6957.
33. Kang, J., Lemaire, H.-G., Unterbeck, A., Salbaum, J. M., Masters, C. L., Grzeschik, K.-H. *et al.* (1987). The precursor of Alzheimer's disease amyloid A4 protein resembles a cell-surface receptor. *Nature,* **325**, 733-736.
34. Sisodia, S. S. (1992). β-amyloid precursor protein cleavage by a membrane-bound protease. *Proc. Natl Acad. Sci. USA,* **89**, 6075-6079.

35. Hashimoto, M. & Masliah, E. (1999). α-synuclein in Lewy body disease and Alzheimer's disease. *Brain Pathol.* **9**, 707-720.
36. Weinreb, P. H., Zhen, W. G., Poon, A. W., Conway, K. A. & Lansbury, P. T., Jr (1996). NACP, a protein implicated in Alzheimer's disease and learning, is natively unfolded. *Biochemistry,* **35**, 13709-13715.
37. Conway, K. A., Harper, J. D. & Lansbury, P. T. (1998). Accelerated *in vitro* fibril formation by a mutant α-synuclein linked to early-onset Parkinson disease. *Nature Med.* **4**, 1318-1320.
38. Narhi, L., Wood, S. J., Steavenson, S., Jiang, Y. J., Wu, G. M., Anafi, D. *et al*. (1999). Both familial Parkinson disease mutations accelerate α-synuclein aggregation. *J. Biol. Chem.* **274**, 9843-9846.
39. Davidson, W. S., Jonas, A., Clayton, D. F. & George, J. M. (1998). Stabilization of α-synuclein secondary structure upon binding to synthetic membranes. *J. Biol. Chem.* **273**, 9443-9449.
40. Perrin, R. J., Woods, W. S., Clayton, D. F. & George, J. M. (2000). Interaction of human alpha-synuclein and Parkinson's disease variants with phospholipids - structural analysis using site-directed mutagenesis. *J. Biol. Chem.* **275**, 34393-34398.
41. Liu, H., Farr-Jones, S., Ulyanov, N. B., Llinas, M., Marqusee, S., Groth, D. *et al*. (1999). Solution structure of Syrian hamster prion protein rPrP(90-231). *Biochemistry,* **38**, 5362-5377.
42. Donne, D. G., Viles, J. H., Groth, D., Mehlhorn, I., James, T. L., Cohen, F. E. *et al*. (1997). Structure of the recombinant full-length hamster prion protein PrP(29-231): the N terminus is highly flexible. *Proc. Natl Acad. Sci. USA,* **94**, 13452-13457.
43. Booth, D. R., Sunde, M., Bellotti, V., Robinson, C. V., Hutchinson, W. L., Fraser, P. E. *et al*. (1997). Instability, unfolding and aggregation of human lysozyme variants underlying amyloid fibrillogenesis. *Nature,* **385**, 787-793.
44. Pan, K. M., Baldwin, M., Nguyen, J., Gasset, M., Serban, A., Groth, D. *et al*. (1993). Conversion of α-helices into β-sheets features in the formation of the scrapie prion proteins. *Proc. Natl Acad. Sci. USA,* **90**, 10962-10966.
45. Perczel, A., Park, K. & Fasman, G. D. (1992). Analysis of the circular dichroism spectrum of proteins using the convex constraint algorithm: a practical guide. *Anal. Biochem.* **203**, 83-93.
46. Venyaminov, S. Y. & Yang, J. T. Y. (1996). Determination of protein secondary structure. In *Circular Dichroism and the Conformational Analysis of Biomolecules* (Fasman, G. D., ed.), pp. 69-107, Plenum Press, New York.
47. Perczel, A. & Hollósi, M. (1996). Turns. In *Circular Dichroism and the Conformational Analysis of Biomolecules* (Fasman, G. D., ed.), pp. 285-380, Plenum Press, New York.
48. Sreerama, N. & Woody, R. W. (2000). Estimation of protein secondary structure from circular dichroism spectra: comparison of CONTIN, SELCON, and CDSSTR methods with an expanded reference set. *Anal. Biochem.* **287**, 252-260.
49. Hendriks, L., van Duijn, C. M., Cras, P., Cruts, M., Van Hul, W., van Harskamp, F. *et al*. (1992). Presenile dementia and cerebral haemorrhage linked to a mutation at codon 692 of the β-amyloid precursor protein gene. *Nature Genet.* **1**, 218-221.
50. Nilsberth, C., Forsell, C., Axelman, K., Gustafsson, C., Luthman, J., Naslund, J. & Lannfelt, L. (1999). A novel APP mutation (E693G)- the Arctic mutation, causing Alzheimer's disease with vascular symptoms. *Soc. Neurosci. Abstr.* **25**, 297.
51. Levy, E., Carman, M. D., Fernandez-Madrid, I. J., Power, M. D., Lieberburg, I., van Duinen, S. G. *et al*. (1990). Mutation of the Alzheimer's disease amyloid gene in hereditary cerebral hemorrhage, Dutch-type. *Science,* **248**, 1124-1126.
52. Bugiani, O., Padovani, A., Magoni, M., Andora, G., Sgarzi, M., Savoiardo, M. *et al*. (1998). An Italian type of HCHWA. *Neurobiol. Aging,* **19**, S238.
53. Fezoui, Y., Hartley, D. M., Walsh, D. M., Selkoe, D. J., Osterhout, J. J. & Teplow, D. B. (2000). A *de novo* designed helix-turn-helix peptide forms nontoxic amyloid fibrils. *Nature Struct. Biol.* **7**, 1095-1099.
54. Lomakin, A., Benedek, G. B. & Teplow, D. B. (1999). Monitoring protein assembly using quasielastic light scattering spectroscopy. In *Amyloid, Prions, and Other Protein Aggregates* (Wetzel, R., ed.), vol. 309, pp. 429-459, Academic Press, San Diego.
55. Lehninger, A. L. (1970), *Biochemistry*, Worth Publishers, New York.
56. Dayhoff, M. O., Barker, W. C. & Hunt, L. T. (1983). Establishing homologies in protein sequences. *Methods Enzymol.* **91**, 524-545.
57. Alzheimer, A. (1906). Über einen eigenartigen schweren Erkrankungsprozeß der Hirnrinde. *Neurol. Centr.* **23**, 1129-1136.
58. Glenner, G. G. & Wong, C. W. (1984). Alzheimer's disease and Down's syndrome: sharing of a unique cerebrovascular amyloid fibril protein. *Biochem. Biophys. Res. Commun.* **122**, 1131-1135.
59. Tanzi, R. E., Gusella, J. F., Watkins, P. C., Bruns, G. A. B., St. George-Hyslop, P. H., Van Keuren, M. L. *et al*. (1987). Amyloid β-protein gene: cDNA, mRNA distribution, and genetic linkage near the Alzheimer locus. *Science,* **235**, 880-884.
60. Goldgaber, D., Lerman, M. I., McBridge, O. W., Saffiotti, V. & Gajdusek, D. C. (1987). Characterization and chromosomal localization of a cDNA encoding brain amyloid of Alzheimer's disease. *Science,* **235**, 877-880.
61. Robakis, N. K., Ramakrishna, N., Wolfe, G. & Wisniewski, H. M. (1987). Molecular cloning and characterization of a cDNA encoding the cerebrovascular and the neuritic plaque amyloid peptides. *Proc. Natl Acad. Sci. USA,* **84**, 4190-4194.
62. Chui, D. H., Tanahashi, H., Ozawa, K., Ikeda, S., Checler, F., Ueda, O. *et al*. (1999). Transgenic mice with Alzheimer presenilin 1 mutations show accelerated neurodegeneration without amyloid plaque formation. *Nature Med.* **5**, 560-564.
63. Hsia, A. Y., Masliah, E., McConlogue, L., Yu, G. Q., Tatsuno, G., Hu, K. *et al*. (1999). Plaque-independent disruption of neural circuits in Alzheimer's disease mouse models. *Proc. Natl Acad. Sci. USA,* **96**, 3228-3233.
64. Moechars, D., Dewachter, I., Lorent, K., Reverse, D., Baekelandt, V., Naidu, A. *et al*. (1999). Early phenotypic changes in transgenic mice that overexpress different mutants of amyloid precursor protein in brain. *J. Biol. Chem.* **274**, 6483-6492.
65. Kumar-Singh, S., Dewachter, I., Moechars, D., Lubke, U., De Jonghe, C., Ceuterick, C. *et al*. (2000). Behavioral disturbances without amyloid deposits in mice overexpressing human amyloid precursor protein with Flemish (A692G) or Dutch (E693Q) mutation. *Neurobiol. Dis.* **7**, 9-22.

66. Mucke, L., Masliah, E., Yu, G. Q., Mallory, M., Rockenstein, E. M., Tatsuno, G. *et al*. (2000). High-level neuronal expression of Aβ(1-42) in wild-type human amyloid protein precursor transgenic mice: Synaptotoxicity without plaque formation. *J. Neurosci.* **20**, 4050-4058.
67. Bouchard, M., Zurdo, J., Nettleton, E. J., Dobson, C. M. & Robinson, C. V. (2000). Formation of insulin amyloid fibrils followed by FTIR simultaneously with CD and electron microscopy. *Protein Sci.* **9**, 1960-1967.
68. Nettleton, E. J., Tito, P., Sunde, M., Bouchard, M., Dobson, C. M. & Robinson, C. V. (2000). Characterization of the oligomeric states of insulin in self-assembly and amyloid fibril formation by mass spectrometry. *Biophysical J.* **79**, 1053-1065.
69. van Beek, J. D., Beaulieu, L., Schafer, H., Demura, M., Asakura, T. & Meier, B. H. (2000). Solid-state NMR determination of the secondary structure of Samia cynthia ricini silk. *Nature,* **405**, 1077-1079.
70. Bales, K. R., Verina, T., Dodel, R. C., Du, Y. S., Altstiel, L., Bender, M. *et al*. (1997). Lack of apolipoprotein E dramatically reduces amyloid β-peptide deposition. *Nature Genet.* **17**, 263-264.
71. Holtzman, D. M., Bales, K. R., Wu, S., Bhat, P., Parsadanian, M., Fagan, A. M. *et al*. (1999). Expression of human apolipoprotein E reduces amyloid-β deposition in a mouse model of Alzheimer's disease. *J. Clin. Invest.* **103**, R15-R21.
72. Lemere, C. A., Blusztajn, J. K., Yamaguchi, H., Wisniewski, T., Saido, T. C. & Selkoe, D. J. (1996). Sequence of deposition of heterogeneous amyloid β-peptides and Apo E in Down syndrome - implications for initial events in amyloid plaque formation. *Neurobiol. Dis.* **3**, 16-32.
73. Iwatsubo, T., Mann, D. M. A., Odaka, A., Suzuki, N. & Ihara, Y. (1995). Amyloid β protein (Aβ) deposition: Aβ42(43) precedes Aβ40 in Down syndrome. *Ann. Neurol.* **37**, 294-299.
74. Pitschke, M., Prior, R., Haupt, M. & Riesner, D. (1998). Detection of single amyloid β-protein aggregates in the cerebrospinal fluid of Alzheimer's patients by fluorescence correlation spectroscopy. *Nature Med.* **4**, 832-834.
75. Walsh, D. M., Lomakin, A., Benedek, G. B., Condron, M. M. & Teplow, D. B. (1997). Amyloid β-protein fibrillogenesis - detection of a protofibrillar intermediate. *J. Biol. Chem.* **272**, 22364-22372.
76. Harper, J. D., Wong, S. S., Lieber, C. M. & Lansbury, P. T. (1997). Observation of metastable Aβ amyloid protofibrils by atomic force microscopy. *Chem. Biol.* **4**, 119-125.
77. Lundberg, K. M., Stenland, C. J., Cohen, F. E., Prusiner, S. B. & Millhauser, G. L. (1997). Kinetics and mechanism of amyloid formation by the prion protein H1 peptide as determined by time-dependent ESR. *Chem. Biol.* **4**, 345-55.
78. Conway, K. A., Lee, S. J., Rochet, J. C., Ding, T. T., Williamson, R. E. & Lansbury, P. T. (2000). Acceleration of oligomerization, not fibrillization, is a shared property of both α-synuclein mutations linked to early-onset Parkinson's disease: implications for pathogenesis and therapy. *Proc. Natl Acad. Sci. USA,* **97**, 571-576.
79. Miller, D. L., Papayannopoulos, I. A., Styles, J. & Bobin, S. A. (1993). Peptide compositions of the cerebrovascular and senile plaque core amyloid deposits of Alzheimer's disease. *Arch. Biochem. Biophys.* **301**, 41-52.
80. Naslund, J., Schierhorn, A., Hellman, U., Lannfelt, L., Roses, A. D.,Tjernberg, L. O. *et al*. (1994). Relative abundance of Alzheimer Aβ amyloid peptide variants in Alzheimer disease and normal aging. *Proc. Natl Acad. Sci. USA,* **91**, 8378-8382.
81. Russo, C., Saido, T. C., DeBusk, L. M., Tabaton, M., Gambetti, P. & Teller, J. K. (1997). Heterogeneity of water-soluble amyloid β-peptide in Alzheimer's disease and Down's syndrome brains. *FEBS Letters,* **409**, 411-416.
82. Russo, C., Violani, E., Salis, S. & Venezia, V. (2000). Neurotoxic and fibrillogenic properties of amino-terminally modified amyloid β-peptides. *Neurobiol. Aging,* **21**, S263.
83. Walsh, D. M., Hartley, D. M., Condron, M. M., Selkoe, D. J. & Teplow, D. B. (2001). *In vitro* studies of amyloid β-protein fibril assembly and toxicity provide clues to the aetiology of Flemish variant ($Ala^{692} \rightarrow Gly$) Alzheimer's disease. *Biochem. J.* **355**, 869-877.
84. Fraser, P. E., Nguyen, J. T., Inouye, H., Surewicz, W. K., Selkoe, D. J., Podlisny, M. B. & Kirschner, D. A. (1992). Fibril formation by primate, rodent, and Dutch-hemorrhagic analogues of Alzheimer amyloid β-protein. *Biochemistry,* **31**, 10716-10723.
85. Wisniewski, T., Ghiso, J. & Frangione, B. (1991). Peptides homologous to the amyloid protein of Alzheimer's disease containing a glutamine for glutamic acid substitution have accelerated amyloid fibril formation. *Biochem. Biophys. Res. Commun.* **179**, 1247-1254.
86. Miravalle, L., Tokuda, T., Chiarle, R., Giaccone, G., Bugiani, O., Tagliavini, F. *et al*. (2000). Substitutions at codon 22 of Alzheimer's Aβ peptide induce diverse conformational changes and apoptotic effects in human cerebral endothelial cells. *J. Biol. Chem.* **275**, 27110-27116.
87. Nilsberth, C., Westlind-Danielsson, A., Eckman, C. B., Condron, M. M., Axelman, K., Forsell, C., Stenh, C. *et al*. (2001). The 'Arctic' APP mutation (E693G) causes Alzheimer's disease by enhanced Aβ protofibril formation. *Nat Neurosci,* **4**, 887-893.
88. Lee, J. P., Stimson, E. R., Ghilardi, J. R., Mantyh, P. W., Lu, Y. A., Felix, A. M. *et al*. (1995). ^{1}H NMR of Aβ amyloid peptide congeners in water solution. Conformational changes correlate with plaque competence. *Biochemistry,* **34**, 5191-5200.
89. Fraser, P. E., Nguyen, J. T., Surewicz, W. K. & Kirschner, D. A. (1991). pH-dependent structural transitions of Alzheimer amyloid peptides. *Biophysical J.* **60**, 1190-1201.
90. Fraser, P. E., McLachlan, D. R., Surewicz, W. K., Mizzen, C. A., Snow, A. D., Nguyen, J. T. & Kirschner, D. A. (1994). Conformation and fibrillogenesis of Alzheimer Aβ peptides with selected substitution of charged residues. *J. Mol. Biol.* **244**, 64-73.
91. Bush, A. I., Pettingell, W. H., Multhaup, G., Paradis, M. D., Vonsattel, J. P., Gusella, J. F. *et al*. (1994). Rapid induction of Alzheimer Aβ amyloid formation by zinc. *Science,* **265**, 1464-1467.
92. Schwarzman, A. L., Gregori, L., Vitek, M. P., Lyubski, S., Strittmatter, W. J., Enghilde, J. J. *et al*. (1994). Transthyretin sequesters amyloid β protein and prevents amyloid formation. *Proc. Natl Acad. Sci. USA,* **91**, 8368-8372.
93. Huang, X. D., Atwood, C. S., Moir, R. D., Hartshorn, M. A., Vonsattel, J. P., Tanzi, R. E. & Bush, A. I. (1997). Zinc-induced Alzheimers Aβ1-40

aggregation is mediated by conformational factors. *J. Biol. Chem.* **272**, 26464-26470.
94. Esler, W. P., Stimson, E. R., Ghilardi, J. R., Lu, Y. A., Felix, A. M., Vinters, H. V. *et al*. (1996). Point substitution in the central hydrophobic cluster of a human β-amyloid congener disrupts peptide folding and abolishes plaque competence. *Biochemistry,* **35**, 13914-13921.
95. McLaurin, J. & Fraser, P. E. (2000). Effect of amino-acid substitutions on Alzheimer's amyloid-β peptide-glycosaminoglycan interactions. *Eur. J. Biochem.* **267**, 6353-6361.
96. Mori, H., Ishii, K., Tomiyama, T., Furiya, Y., Sahara, N., Asano, S. *et al*. (1994). Racemization: its biological significance on neuropathogenesis of Alzheimer's disease. *Tohoku J. Exp. Med*. **174**, 251-262.
97. Tomiyama, T., Asano, S., Furiya, Y., Shirasawa, T., Endo, N. & Mori, H. (1994). Racemization of Asp^{23} residue affects the aggregation properties of Alzheimer amyloid β protein analogues. *J. Biol. Chem.* **269**, 10205-10208.
98. Shimizu, T., Izumiyama, N., Murayama, S., Fukuda, H. & Shirasawa, T. (2000). Aggregation and fibril formation of mutant or isomerised forms of the amyloid β-proteins. *Soc. Neurosci. Abstr.* **26**, 1284.
99. Grabowski, T. J., Cho, H. S., Vonsattel, J. P. G., Rebeck, G. W. & Greenberg, S. M. (2001). Novel amyloid precursor protein mutation in an Iowa family with dementia and severe cerebral amyloid angiopathy. *Ann. Neurol.* **49**, 697-705.
100. Chu, H. L. & Lin, S. Y. (2001). Temperature-induced conformational changes in amyloid β(1-40) peptide investigated by simultaneous FT-IR microspectroscopy with thermal system. *Biophys. Chem.* **89**, 173-180.
101. Dobson, C. M., Evans, P. A. & Radford, S. E. (1994). Understanding how proteins fold - The lysozyme story so far. *Trends Biochem. Sci.* **19**, 31-37.
102. Kuwajima, K. (1996). Stopped-flow circular dichroism. In *Circular Dichroism and the Conformational Analysis of Biomolecules* (Fasman, G. D., ed.), pp. 159-182, Plenum Press, New York.
103. Harrison, P. M., Bamborough, P., Daggett, V., Prusiner, S. B. & Cohen, F. E. (1997). The prion folding problem. *Curr. Opin. Struct. Biol.* **7**, 53-59.
104. Mihara, H. & Takahashi, Y. (1997). Engineering peptides and proteins that undergo α-to-β transitions. *Curr. Opin. Struct. Biol.* **7**, 501-508.
105. Takahashi, Y., Yamashita, T., Ueno, A. & Mihara, H. (2000). Construction of peptides that undergo structural transition from α-helix to β-sheet and amyloid fibril formation by the introduction of N-terminal hydrophobic amino acids. *Tetrahedron,* **56**, 7011-7018.
106. Kallberg, Y., Gustafsson, M., Persson, B., Thyberg, J. & Johansson, J. (2001). Prediction of amyloid fibril-forming proteins. *J. Biol. Chem.* **276**, 12945-12950.
107. Lomakin, A., Chung, D. S., Benedek, G. B., Kirschner, D. A. & Teplow, D. B. (1996). On the nucleation and growth of amyloid β-protein fibrils: Detection of nuclei and quantitation of rate constants. *Proc. Natl Acad. Sci. USA,* **93**, 1125-1129.
108. Fezoui, Y., Hartley, D. M., Harper, J. D., Khurana, R., Walsh, D. M., Condron, M. M. *et al*. (2000). An improved method of preparing the amyloid β-protein for fibrillogenesis and neurotoxicity experiments. *Amyloid,* **7**, 166-178.
109. Brahms, S. & Brahms, J. (1980). Determination of protein secondary structure in solution by vacuum ultraviolet circular dichroism. *J. Mol. Biol.* **138**, 149-178.
110. Sreerama, N., Venyaminov, S. Y. & Woody, R. W. (2000). Estimation of protein secondary structure from circular dichroism spectra: Inclusion of denatured proteins with native proteins in the analysis. *Anal. Biochem.* **287**, 243-251.

Edited by F. Cohen

(Received 9 March 2001; received in revised form 12 June 2001; accepted 20 July 2001)